Journal of Nanobiotechnology

METHODOLOGY Open Access

Fusiform nanoparticle boosts efficient genetic transformation in *Sclerotinia sclerotiorum*

Yijuan Ding[1,2†], Nan Yang[1,2†], Yi Lu[3], Jiming Xu[3], Kusum Rana[1,2], Yangui Chen[1,2], Zhigang Xu[3], Wei Qian[1,2*] and Huafang Wan[1,2*]

Abstract

Background *Sclerotinia sclerotiorum* is a highly destructive phytopathogenic fungus that poses a significant threat to a wide array of crops. The current constraints in genetic manipulation techniques impede a thorough comprehension of its pathogenic mechanisms and the development of effective control strategies.

Results Herein, we present a highly efficient genetic transformation system for *S. sclerotiorum*, leveraging the use of fusiform nanoparticles, which are synthesized with $FeCl_3$ and 2,6-diaminopyrimidine (DAP). These nanoparticles, with an average longitude length of 59.00 nm and a positively charged surface, facilitate the direct delivery of exogenous DNA into the mycelial cells of *S. sclerotiorum*, as well as successful integration with stable expression. Notably, this system circumvents fungal protoplast preparation and tedious recovery processes, streamlining the transformation process considerably. Furthermore, we successfully employed this system to generate *S. sclerotiorum* strains with silenced oxaloacetate acetylhydrolase-encoding gene *Ss-oah1*.

Conclusions Our findings demonstrate the feasibility of using nanoparticle-mediated delivery as a rapid and reliable tool for genetic modification in *S. sclerotiorum*. Given its simplicity and high efficiency, it has the potential to significantly propel genetic research in filamentous fungi, offering new avenues for elucidating the intricacies of pathogenicity and developing innovative disease management strategies.

Keywords Fusiform nanoparticle, *Sclerotinia sclerotiorum*, Gene silencing, Mycelium transformation, *Ss-oah1*

Introduction

Fungal diseases are a major menace to crop yield, responsible for annual losses ranging among 10-23%, along with an additional 10-20% post-harvest loss [1, 2]. These challenges are expected to intensify with the evolving climate [3]. Among the myriad of pathogens, the ascomycete *Sclerotinia sclerotiorum* (Lib.) de Bary is particularly notorious for its destructive and widespread impact. It can infect over 600 plant species, encompassing crucial crops like rapeseed and soybean [4]. Its unique dual feeding lifestyle, exhibiting characteristics of both biotroph and necrotroph, makes it a valuable subject for host-pathogen interaction studies [5]. Due to the considerable impact of *S. sclerotiorum* on crops yield and quality, it is imperative to conduct extensive research to identify the function of the genes involved [6]. Elucidating the roles of genes involved in pathogenicity and fungal development is fundamental for unearthing potential targets in disease management. This understanding relies heavily

†Yijuan Ding and Nan Yang contributed to this work equally.

*Correspondence:
Wei Qian
qianwei6666@hotmail.com
Huafang Wan
wanhua05@swu.edu.cn

Full list of author information is available at the end of the article

Graphical Abstract

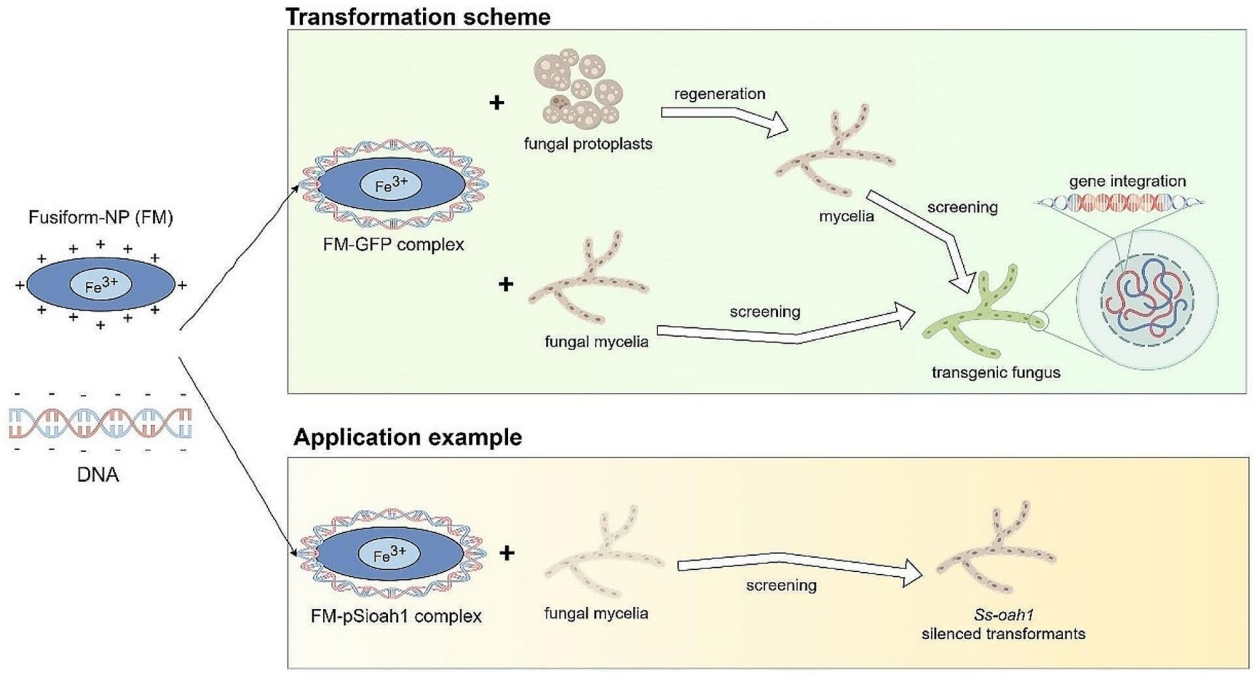

on the availability of an efficient genetic transformation system.

The primary techniques for genetic transformation in filamentous fungi include *Agrobacterium tumefaciens* (AT)- and polyethylene glycol (PEG)-mediated protoplast transformation, along with electroporation [7]. In the case of *S. sclerotiorum*, protoplast transformations mediated by PEG or AT have been successfully applied for gene transfer, gene knock-out, and insertional mutagenesis [8, 9]. Despite their utility, these methods have their drawbacks, including relatively low transformation rate, the need for precise osmotic balance, and the delicate and laborious handling and regeneration of protoplasts involved in the gene transfer process [7]. Biolistic transformation presents an alternative by delivering exogenous DNA into fungal spores or hyphae via microscopic particles [7]. However, the efficacy of this approach hinges on several critical factors, including the specificity of particle delivery apparatus, the type and density of target cells, the osmotic environment, and the methodology employed for particle coating [10, 11]. Shock wave-mediated transformation has emerged as an effective technique for some filamentous fungi [12]. It transiently modulates the permeability of fungal cell membranes, facilitating the entry of DNA with a high degree of reproducibility [13]. Nonetheless, the application of this method is impeded by the high costs of the shock wave sources and the specialized equipment required [13].

Nanomaterials have attracted significant interest for their role in delivering biological molecules into animal cells, leveraging their small size, large surface area, compatibility with biological systems, degradability, and low toxicity [14]. However, their use in plant cells faces the challenge posed by the robust cell wall, which acts as a natural barrier to nanoparticle penetration. Despite this, recent research has managed to overcome this hurdle, achieving successful delivery of DNA, RNA, and proteins into plant cells [15–28]. All the successful examples refuted the notion of the plant cell wall as an impenetrable barrier. The size, shape, compactness, stiffness of the nanomaterials contributes the ability to penetrate cell walls and internalize into plant cells [29, 30]. Similar to plant cells, the fungal pathogens' cells are enveloped by a resilient cell wall. However, only two studies have reported the application of nanomaterials in successfully transferring exogenous DNA into fungal cell, such as yeast and *Candida albicans* [31, 32].

In our previous research, a kind of nanoparticle with fusiform morphology (FDAP-NP), synthesized with 2,6-diaminopyridine and Fe^{3+}, possesses good permeability in solid tumors and can load drug doxorubicin to enhance thermal therapy and chemotherapy to tumor [33]. Base on its good permeability, we hypothesized that it may easily penetrate fungal cell. Therefore, this kind of fusiform nanoparticle (Fusiform-NP, FM) was resynthesized in this research with some modification and chosen as the carrier for the integration of exogenous DNA into

the genome of *S. sclerotiorum* through either protoplast or mycelium transformation. We loaded a GFP expression construct onto the FM and successfully obtained the strains with green fluorescence via FM-mediated protoplast or mycelium transformation. Meanwhile, in order to verify the feasibility of FM-mediated mycelium transformation in gene function analysis of *S. sclerotiorum*, we transferred a gene-silencing vector to silence the oxaloacetate acetylhydrolase gene (*Ss-oah1*) [34]. The study highlights a much more convenient approach to the mycelium transformation and confirms the FM is non-toxic to *S. sclerotiorum*.

Materials and methods

Pathogenicity analysis of *S. sclerotiorum*

The *S. sclerotiorum* wild type strain 1980 (WT) and the transformants were routinely stored and cultured on potato dextrose agar media (PDA, 20% potato, 2% dextrose and 1.5% agar) (Macklin, Shanghai, China) at 22 °C [35]. *Brassica napus* (rapeseed) and *Glycine max* (soybean) were cultivated in the field according to the routine cultivation and management measures in Beibei, Chongqing, China. *Nicotiana benthamiana* (tobacco) was grown in the autoclaved medium (Pindstrup, Fabriksvej, Danmark) in climate chamber at the cycle of 28 ± 2 °C with 16 h light and 16 ± 2 °C with 8 h dark, under 70% relative humidity. To assess the pathogenicity of the transformed strains of *S. sclerotiorum*, detached leaves of rapeseed, soybean, and tobacco were inoculated with mycelia agar plugs (6 mm in diameter) at 22 ± 1 °C under approximate 95% relative humidity. The lesion size was calculated at 48 h post inoculation (hpi). Each experiment was performed in triplicate.

Preparation of FM-DNA complexes

The pEF1-GFP construct was generated by the insertion of the codon-optimized gene encoding Green Fluorescent Protein (GFP) into the pUC57 cloning vector [36], driven by the promoter of elongation factor 1 alpha (EF1α, SS1G_05520). The fragment of *S. sclerotiorum Ss-oah1* was amplified using the primer pair Sioah-F and Sioah-R (Supplementary Table S1). The amplicons were then inserted into the corresponding multiple cloning sites of vector pCIT, constructing the gene-silencing vector pSioah1, following the protocol previously outlined [37]. The FM was synthesized according to the previous study with some modification [33]. Briefly, 24.0 mmol of $FeCl_3{\cdot}6H_2O$ was completely dissolved in 120 mL of double-distilled water followed by oxygen-removal with argon for 1 h, and then was mixed with 6.0 mmol of DAP (2,6-diaminopyrimidine) to polymerize FMs at 50 °C for 24 h. The synthesized product subsequently underwent purification via dialysis using a 3,500 Da molecular weight cutoff dialysis bag submerged in sterile distilled water at ambient temperature for 24 h. The purified FMs were thereafter preserved at 4 °C for the following use.

To confirm the indeed penetration of the nanoparticles through the cell wall of *S. sclerotiorum*, the FM was labelled with indocyanine Green (ICG), designated as FM^{ICG} (FMI). ICG emits red fluorescence at the wavelength of 785 nm, which can be detected using confocal microscopy (LSM800, ZEISS, Germany). For the preparation of FM-DNA or FMI-DNA complexes, plasmid was incubated with FMs or FMIs in a sterile centrifuge tube with a mass ratio of 1:400 and shaken overnight on an oscillatory table (OS-200, Hangzhou, China) at 50 rpm at room temperature. The mixture was then centrifuged (Micro-17, Thermo, Massachusetts, USA) at 5,000 rpm for 10 min to remove the unbound DNA. Diluted sample (10 μL) (FM or FM-DNA) was evenly dispersed on a hydrophilicity-treated copper grid and dried in a vacuum desiccator (Sigma-Aldrich (Shanghai), Shanghai, China) at room temperature. This process was repeated 5 to 6 times to amass a sufficient sample for morphology characterization using transmission electron microscope (TEM, HT7800, HITACHI, Japan) (HC-1, Accelerating voltage = 80,000; Magnification = 70,000; Spot number = 5; Emission = 10). The particle size distribution and charge on the surface were tested through dynamic light scattering (DLS) and zeta potential analysis, respectively [38]. The stability of FM-DNA complexes was periodically evaluated with DLS and polymer dispersity index (PDI), which were conducted bi-daily throughout the storage period [38].

FM-mediated transformation in *S. sclerotiorum*

The protoplast of *S. sclerotiorum* was prepared following the protocol described by Rollins [39]. Briefly, the harvested mycelia of *S. sclerotiorum* cultured on the PDA medium (90 mm in diameter) after 36 h incubation were treated with a solution comprising snailase (1 $mg{\cdot}mL^{-1}$) (Solarbio, Beijing, China) and megalyase (10 $mg{\cdot}mL^{-1}$) (Shenqi Biotechnology, Shanghai, China) at 30 °C for 4 h to digest the cell wall. The protoplasts were collected through filtration and washed with 0.8 M $MgSO_4$ to remove any residual enzymes, followed by resuspension in a STC solution (QualityYard, Beijing, China). Two-hundred microliters of FM-DNA complexes were incubated with 100 μL *S. sclerotiorum* protoplasts (approximately 10^3 protoplasts$\cdot\mu L^{-1}$) in a sterile centrifuge tube at room temperature for 2 h, followed by centrifugation at 4,000 rpm for 3 min to collect the transformed-protoplasts. The pelleted transformed-protoplasts were then washed twice with 0.01 M phosphate buffer solution (PBS, 8.00 g NaCl, 0.20 g KCl, 1.44 g Na_2HPO_4, 0.24 g KH_2PO_4 in 1 L distilled water, pH = 7.40). Subsequently, the transformed protoplasts were resuspended on cell wall recovery medium (47.92 g

sucrose, 0.10 g yeast extract, 0.10 g lactium, 2.40 g agar in 1 L distilled water). After cell wall reconstruction, the cells were transferred to the selective medium (PDA supplemented with 100 $mg{\cdot}L^{-1}$ hygromycin (Sigma-Aldrich (Shanghai), Shanghai, China)) for the screening and proliferation of transformants. Parallel to this, the entire *S. sclerotiorum* mycelia cultured on the PDA medium (90 mm in diameter) after 2 days incubation, were directly incubated with 4 mL FM-DNA complexes (FM-DNA:0.01 M PBS = 1:3) at room temperature for 3 h. After incubation, the extra FM-DNA complexes were rinsed out with 0.01 M PBS for 3–5 times and then the mycelia with fluorescence signal were selected and transferred onto the selective medium. The process for selecting and cultivating transformants was consistent with the aforementioned methods.

The transformants obtained through protoplast or mycelium transformation were hyphal tipped and transferred onto the selective medium and screened and cultured up to the fourth generation (T_4). GFP expression within the hyphae was monitored using confocal microscopy across T_1, T_2, T_3, and T_4 generations. Mycelial radial growth was quantified at 12, 24, and 36 hpi on the PDA medium. Mycelial morphology was examined at 3, 5, and 15 days post inoculation (dpi). The average number and dry weight of sclerotia per plate was counted at 15 dpi. The experiments were repeated three times.

Validation of the insertion of exogenous DNA into the genome of *S. sclerotiorum*

Purified genomic DNA was extracted from the mycelia of a putative transformant from T_1 generation with cetyltrimethyl ammonium bromide (CTAB) following the standard procedure [40]. Subsequent polymerase chain reaction (PCR) analysis employing specific primers GFT-F/GFT-R (Supplementary Table S1) was performed to validate positive transformants. Furthermore, the precise genomic integration site of the exogenous DNA within *S. sclerotiorum* genome was determined through genome re-sequencing using the Illumina HiSeq platform employing the Sequencing by Synthesis (SBS) (Beijing Biomics Biotech Co. Ltd.). Raw data quality control assessments were performed using FastQC, and high-quality sequences were isolated following the removal of adaptor sequences and low-quality reads (including reads with a proportion of N greater than 10%; reads with a mass value of Q (Quality Score) ≤ 10 with an alkali base accounting for more than 50% of the entire Read). The clean reads of the transformant were assembled and aligned to the reference genome of *S. sclerotiorum* 1980 (GenBank: GCA_000146945.2) using the Adaptive Insertion Mapping with Sequencing (AIM-Seq) method [41]. Finally, insertion sites of the sequence were conclusively verified by PCR with specific primers TL_F1/ TR_R2 (Supplementary Table S1). PCR reaction program comprised of 94 °C for 3 min (1 cycle), then 94 °C for 30 s, 56 °C for 30 s and 72 °C for 30 s (35 cycles), followed by 72 °C for 3 min.

The expression level of *GFP* and *Ss-oah1* in *S. sclerotiorum* transformants were quantified using the CFX96™ Real-Time PCR system (Bio-Rad, Hercules, CA, USA). Total RNA was extracted from the mycelium using TRIzol reagent (TianGen, Dalian, China) and reversely transcribed into cDNA using the iScript™ cDNA Synthesis Kit (Bio-Rad, California, USA) following the corresponding instructions. The quantitative real-time PCR (qRT-PCR) was performed in triplicate for each gene, using *SsTubulin* (SS1G_04652) encoding tubulin protein as internal standard. The corresponding program was set as follows: predenaturation at 95 °C for 30 s, denaturation at 95 °C for 5 s, annealing at 58–60 °C for 1 min, extension at 72 °C for 20 s. This cycle was repeated for 40 times. The primer sequences used for qRT-PCR are listed in Supplementary Table S1. Preprocessing of the raw data was undertaken using CFX Manager™ v 3.0 (Bio-Rad, California, USA) and the relative expression of target genes was determined with the $2^{-\Delta\Delta CT}$ method [42]. All experiments were conducted in triplicate.

Generating *Ss-oah1*- silenced transformants via FM-mediated mycelium transformation

To investigate the efficacy of FM-mediated mycelium transformation in *S. sclerotiorum*, *Ss-oah1* gene-silencing plasmid, pSioah1, was introduced into *S. sclerotiorum* via mycelium transformation. The *Ss-oah1*-silenced transformants were cultured on PDA media supplemented with 50 $mg{\cdot}L^{-1}$ bromophenol (Macklin, Shanghai, China), which is utilized as an indicator monitoring the qualitative assessment of oxalic acid (OA) production, as the medium shifts to violet (at pH > 4.6) or yellow (at pH < 3.0), depending on the acid produced by *S. sclerotiorum* strains. Quantitative determination of OA production was subsequently performed using high performance liquid chromatography (HPLC) [43]. Specifically, three mycelium plugs (9 mm in diameter) of each transformant were inoculated into 50 mL of potato dextrose broth (PDB, 20% potato, 2% dextrose) (Macklin, Shanghai, China) and incubated at 22 °C with constant agitation at 150 rpm for 3 d. OA concentrations was designated as milligrams of OA per milliliter PDB solution. Three replicates were performed for each transformant.

Statistical analysis

The data from different biological treatments were subjected to one-way analysis of variance (ANOVA) and statistically analyzed using Prism 8 (GraphPad Software, Santiago, USA). The results were presented as the mean

value±standard deviation (SD). Significant difference was calculated using Student's *t*-test (**$P<0.001$).

Results

Characteristics of FM and FM-DNA complex

The FM-DNA complexes were assembled by loading plasmid DNA onto the surface of FM (Fig. 1). The characteristics of FM and FM-DNA complexes were investigated by TEM, DLS and zeta potential analysis. As shown in Fig. 2A, FMs and different FM-DNA complexes displayed a regular, elongated fusiform and uniform morphology. Specifically, the diameter of FM-GFP (FMG, average longitudinal length 70 nm and latitudinal length 30 nm) was marginally larger than those of FM (average longitudinal length 59 nm and latitudinal length 23 nm). DLS and PDI analyses indicated that the average hydrodynamic diameter of FM (average 24.9 nm) was less than that of different FM-DNA complexes (FMI, 46.7 nm; FMG, 41.2 nm; FM^{ICG}-GFP [FMIG], 46.5 nm) (Fig. 2B), which may be attributable to the addition of ICG or DNA to the surface of the nanoparticles. Similar PDI among the FM and the FM-DNA complexes suggested that the loading DNA or ICG did not significantly affect the disperity uniformity. As shown in Fig. 2C, zeta potential analysis showed positive values for different FM-DNA complexes (FMI, +12.6 mV; FMG, +23.0 mV; FMIG, +8.9 mV), but these were lower than that of free nanomaterial particle (average about+44 mV). This implies that the loading of negative DNA or ICG partially neutralized the positive charge on the surface of the nanomaterials. The stability of FMG was assessed by measuring DLS and PDI every two days in one-week storage at room temperature. The dynamics of DLS and PDI revealed no significant fluctuation in diameter and PDI throughout the 7-day period, suggesting robust binding between the DNA and FMs, which conferred substantial stability to the FM-DNA complexes (Fig. 2D).

Delivering exogenous DNA into *S. sclerotiorum* protoplasts via FM

The temporal and spatial distribution of FM and FMG complexes within *S. sclerotiorum* were tracked using confocal fluorescent microscopy at 488 nm wavelength. After 2 h incubation of FMI with *S. sclerotiorum* protoplasts,

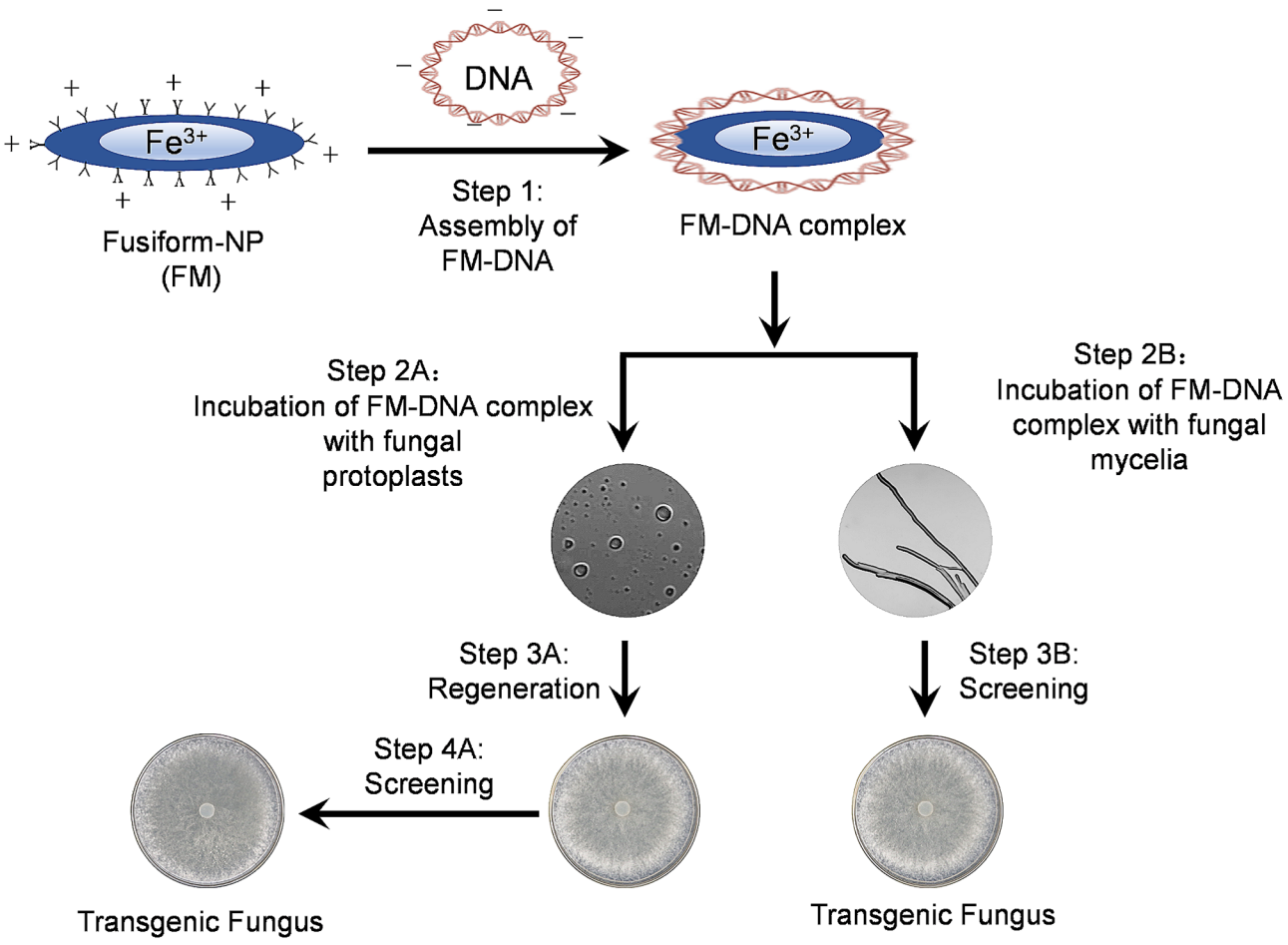

Fig. 1 Schematic illustration of FM-mediated transformation strategy in *S. sclerotiorum*

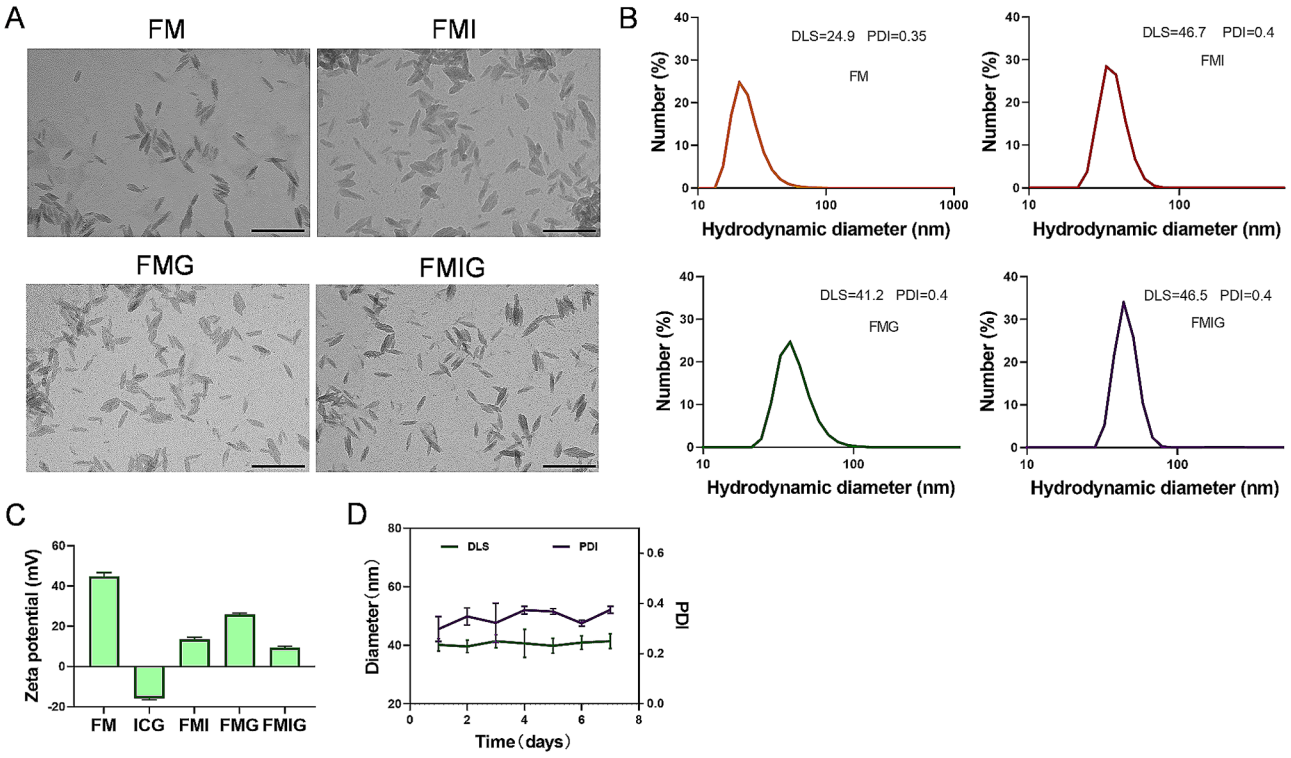

Fig. 2 Characteristics of FM and FM-DNA complexes. **A**: TEM images of FM, FMI, FMG and FMIG complexes. FM, free nanoparticle; FMI, ICG tagged-nanoparticle; FMG, nanoparticle loaded with the plasmid pEF1-GFP; FMIG, ICG tagged-nanoparticle loaded with the plasmid pEF1-GFP. Scale bars, 100 μm. **B**: Hydrodynamic diameter of FM and FM-DNA complexes. DLS, dynamic light scattering; PDI, polymer dispersity index. **C**: zeta potential of FM and FM-DNA complexes. Error bars represent SD from three replicates. **D**: Stability of FMG complexes. Error bars represent SD from three replicates

75.0% of protoplasts exhibited red fluorescence, signifying the successful permeation of FMI into the cells (Fig. 3A). Simultaneously, transformation of pEF1-GFP plasmid into *S. sclerotiorum* protoplasts was attempted utilizing both FM and FMI as vectors. The results indicated that 75.6% of the protoplasts displayed green fluorescence following transformation with the FMG complexes, whereas 68.6% of the protoplasts exhibited dual fluorescence (green and red) after transformation with the FMIG complexes (Fig. 3A). However, *S. sclerotiorum* transformed solely with FM or the pEF1-GFP plasmid did not exhibit green fluorescence (Fig. 3A). Protoplasts transformed with FMG were cultured, yielding mycelial growth exhibiting green fluorescence (T_1 generation) (Fig. 3B). Selective culture of intensely fluorescent mycelia continued over successive generations (T_2, T_3, and T_4) via hyphal-tipping culture. The green fluorescence was constantly observed in T_2, T_3, and T_4 generations upon re-culturing (Fig. 3B). Molecular validation of GFP integration within the *S. sclerotiorum* genome was conducted by PCR analysis, employing the genomic DNA of T_1, T_2, T_3, and T_4 transgenic *S. sclerotiorum* as templates. The presence of PCR amplification products matching the expected length of 250 base pairs was consistent with the observed fluorescence, affirming the success of genetic transformation (Fig. 3C). Furthermore, the *GFP* expression level in T_1, T_2, T_3, and T_4 transgenic *S. sclerotiorum* validated by qRT-PCR further confirmed the internalization of the *GFP* in *S. sclerotiorum* genome (Fig. 3D). Collectively, these results endorse the efficacy of FM in mediating the transfer and stable integration of exogenous DNA into *S. sclerotiorum* via protoplast incubation.

Delivering exogenous DNA into *S. sclerotiorum* mycelia by FM

The successful transformation in protoplast of *S. sclerotiorum* mediated by FM does not offset the relative pitfalls including time-consuming, and complicated manipulation. To streamline this procedure, we explored direct incubation methods. *S. sclerotiorum* mycelia (cultivated for 2 d) were directly incubated with the FMI for 3 h, after which the fluorescence in mycelia was assessed. As anticipated, red fluorescence was detected among transformed *S. sclerotiorum* mycelia (Fig. 4A), indicating the FMI could successfully penetrate the cell wall and the plasmalemma of *S. sclerotiorum* mycelia without any external assistance. Likewise, green fluorescence was observed in the *S. sclerotiorum* mycelia incubated with FMG and FMIG (Fig. 4A). Additionally, we observed that

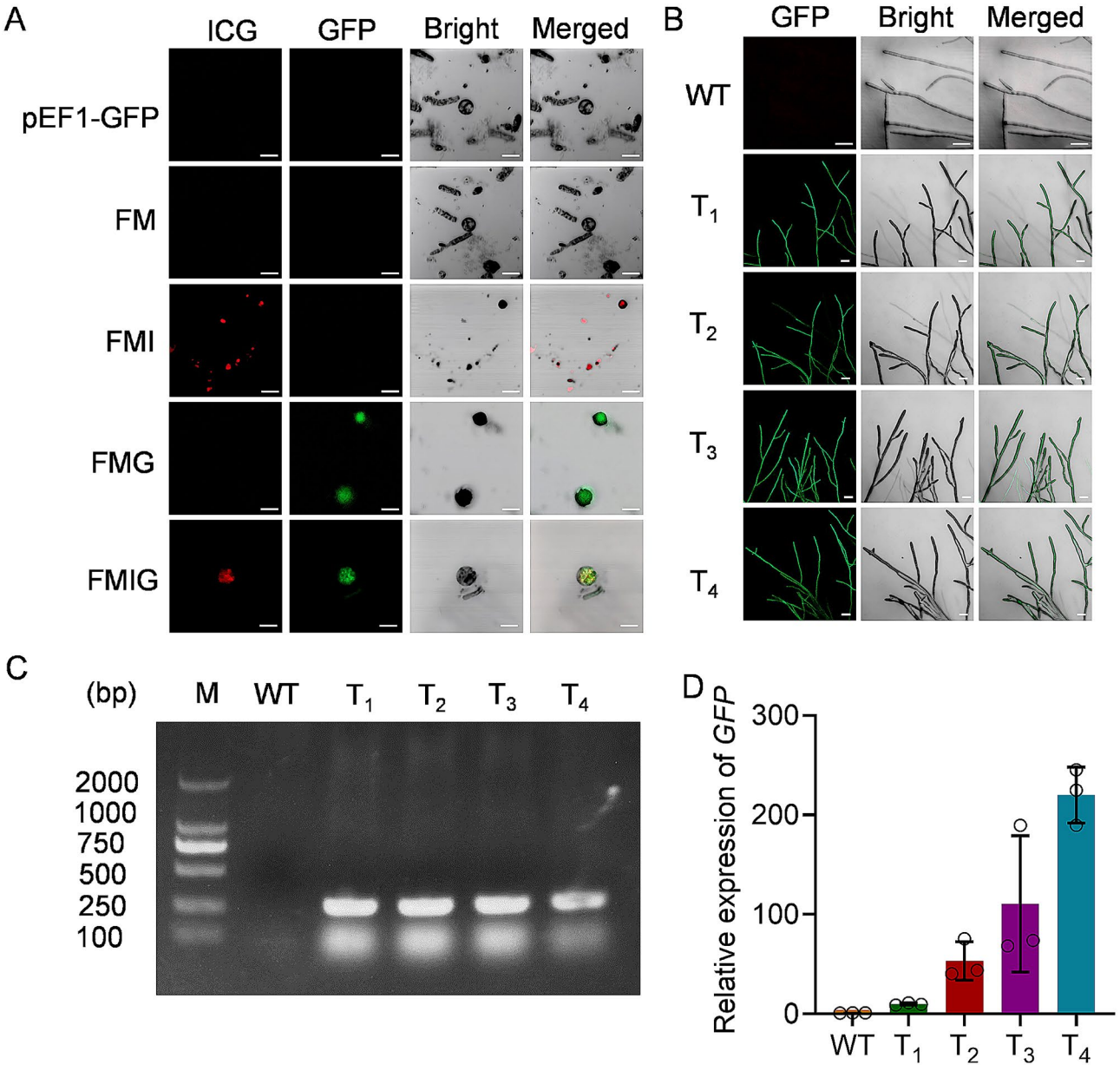

Fig. 3 DNA delivery into protoplasts with FM transformation. **A**: FM internalization into *S. sclerotiorum* protoplasts and tracking of fluorescence in protoplasts via confocal microscopy. Scale bars, 10 μm. **B**: Tracking of green fluorescence in the regenerated *S. sclerotiorum* hyphae and the hyphae of re-cultured generations. *S. sclerotiorum* protoplasts were re-walled to generate T_1 generation, and subsequently re-cultured to generate T_2, T_3 and T_4 generations. WT, wild type strain. Scale bars, 100 μm. **C**: Amplifying *GFP* from transgenic *S. sclerotiorum*. M, DNA ladder; T_1-T_4, T_1 to T_4 generation of transformant. **D**: qRT-PCR analysis of transgenic *S. sclerotiorum*. *Sstubulin* was used as the internal standard. Error bars represent SD from three replicates

the exogenous *GFP* was stably expressed across T_1-T_4 generations derived from the FMG-mediated mycelium transformant via hyphal-tipping culture (Fig. 4B, C).

Genome re-sequencing was employed in the strain from the T_1 generation to ascertain the precise locational integration of the pEF1-GFP construct within the *S. sclerotiorum* genome. A total of 2,652,632,200 bases comprising 8,838,774 pair-end clean reads were obtained (SRA: PRJNA1126013). The GC content of clean reads was approximately 49.56%, with 92.01% clean reads with Q value≥to 30. Junction reads, which include sequences from both the *S. sclerotiorum* reference genome and the inserted exogenous DNA sequence, were utilized for clustering. The results showed that two fragments of pEF1-GFP construct were integrated within the genome of *S. sclerotiorum* (Fig. 4D). Specifically, the insert fragment 1 (6557 bp) covering the entire expression cassette of *GFP* and hygromycin resistance gene (hygromycin-phosphtolransferase, *hph*) was inserted into Chromosome NW_001820820.1 (977055.977062) with six-base

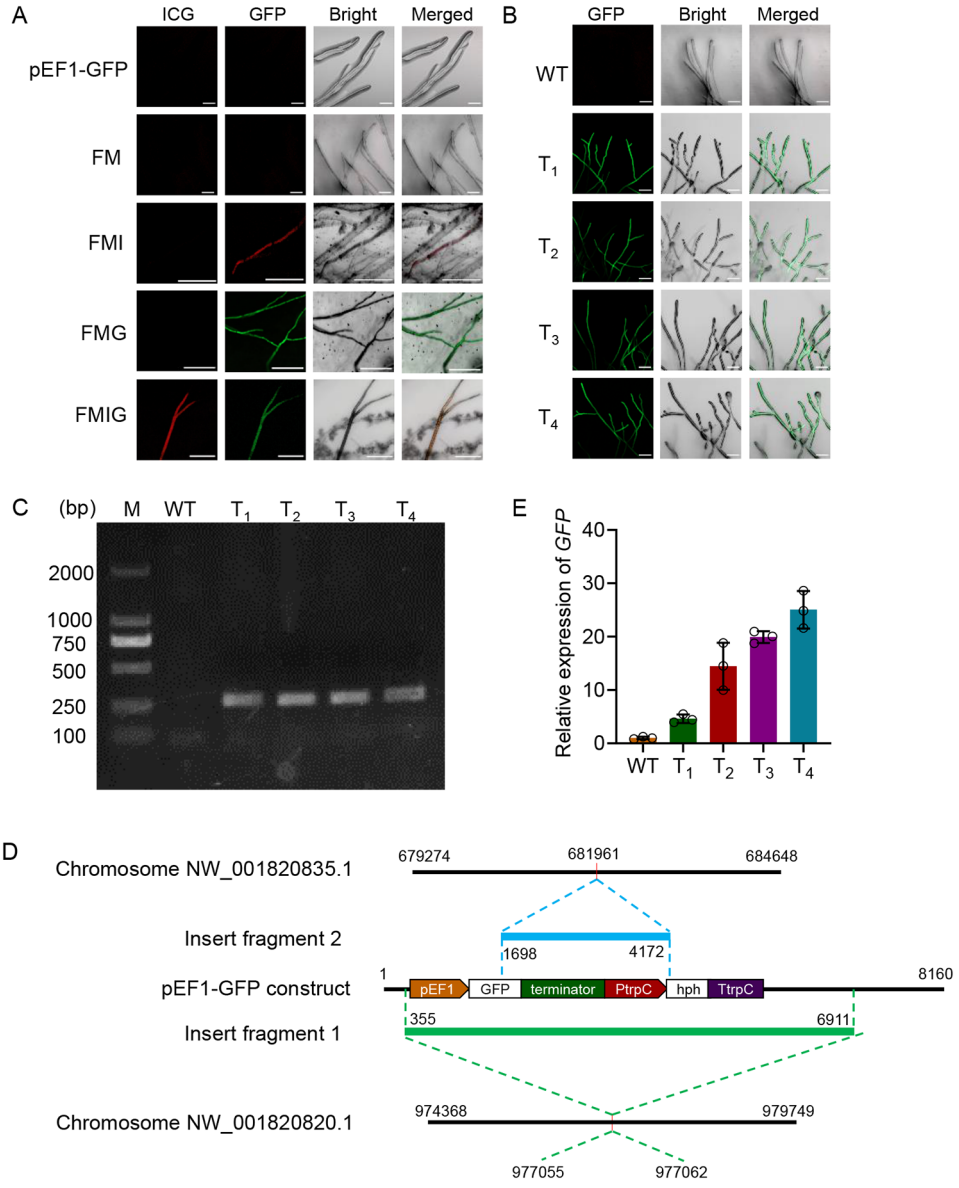

Fig. 4 DNA delivery into *S. sclerotiorum* mycelium with FM transformation platform. **A**: FM internalization into *S. sclerotiorum* mycelium and tracking of fluorescence in mycelia via confocal microscopy. Scale bars, 100 μm. **B**: Tracking of green fluorescence in the re-cultured *S. sclerotiorum* generations. WT, wild type strain. T_1-T_4, transgenic hyphae. Scale bars, 100 μm. **C**: Amplifying of *GFP* from transgenic *S. sclerotiorum*. bp, base pair; M, DNA ladder. **D**: Genome re-sequencing revealed the integration sites in the transgenic *S. sclerotiorum* genome. hph: Hygromycinphosphtolransferase. **E**: qRT-PCR analysis of transgenic *S. sclerotiorum*. *Sstubulin* was used as the internal standard. Error bars represent SD from three replicates

pairs' deletion in *S. sclerotiorum* genome (Fig. 4D). The insert fragment 2 (2475 bp) covering part of the expression cassette of *GFP* and *hph* was inserted into Chromosome NW_001820835.1 (681,961) (Fig. 4D). The green fluorescence and the *GFP* expression were detected among four generations, indicating that the insert fragment 1 was functional. Subsequently, we further validated the insertion site 1 via PCR with two pairs of primers specifically designed to amplify the genomic regions flanking the integration locus. Sequencing analyses confirmed the stable integration of pEF1-GFP in the genomes of T_2, T_3, and T_4 generations (Supplementary Figs. 1, 2). qRT-PCR analysis was further performed among the WT, T_1, T_2, T_3, and T_4 generations, detecting high expression of *GFP* gene in transgenic *S. sclerotiorum* strains (Fig. 4E). Collectively, these findings underscore the capability of FM to directly and efficaciously mediate the transformation and stable genomic integration of exogenous genes in *S. sclerotiorum* via mycelia transformation.

To evaluate the potential cytotoxicity of nanomaterials on *S. sclerotiorum*, the physiological characteristics were compared between WT and T_4 generation. The mycelia

of the transgenic strain showed no significant difference from that of the WT strain at 3, 5, and 15 dai (Fig. 5A). The colony area (cm^2) of the transgenic strains was measured at 12 h, 24 h and 36 h. No significant difference was detected in hyphal growth rate between the transgenic *S. sclerotiorum* strains and WT ($P>0.05$) (Fig. 5B). At 25 dai, no significant variance was detected in the average number of sclerotia ($P=0.4676$) and sclerotia dry weight per plate ($P=0.4414$) between the transgenic *S. sclerotiorum* and the WT strain (Fig. 5C). Moreover, there were no significant differences in the size of the lesions on leaves of rapeseed ($P=0.1875$) inoculated with the transgenic *S. sclerotiorum* and WT strain, as well as that in leaves of soybean ($P=0.6887$) and tobacco ($P=0.4925$) (Fig. 5D, E). These results indicated that the FM exerted

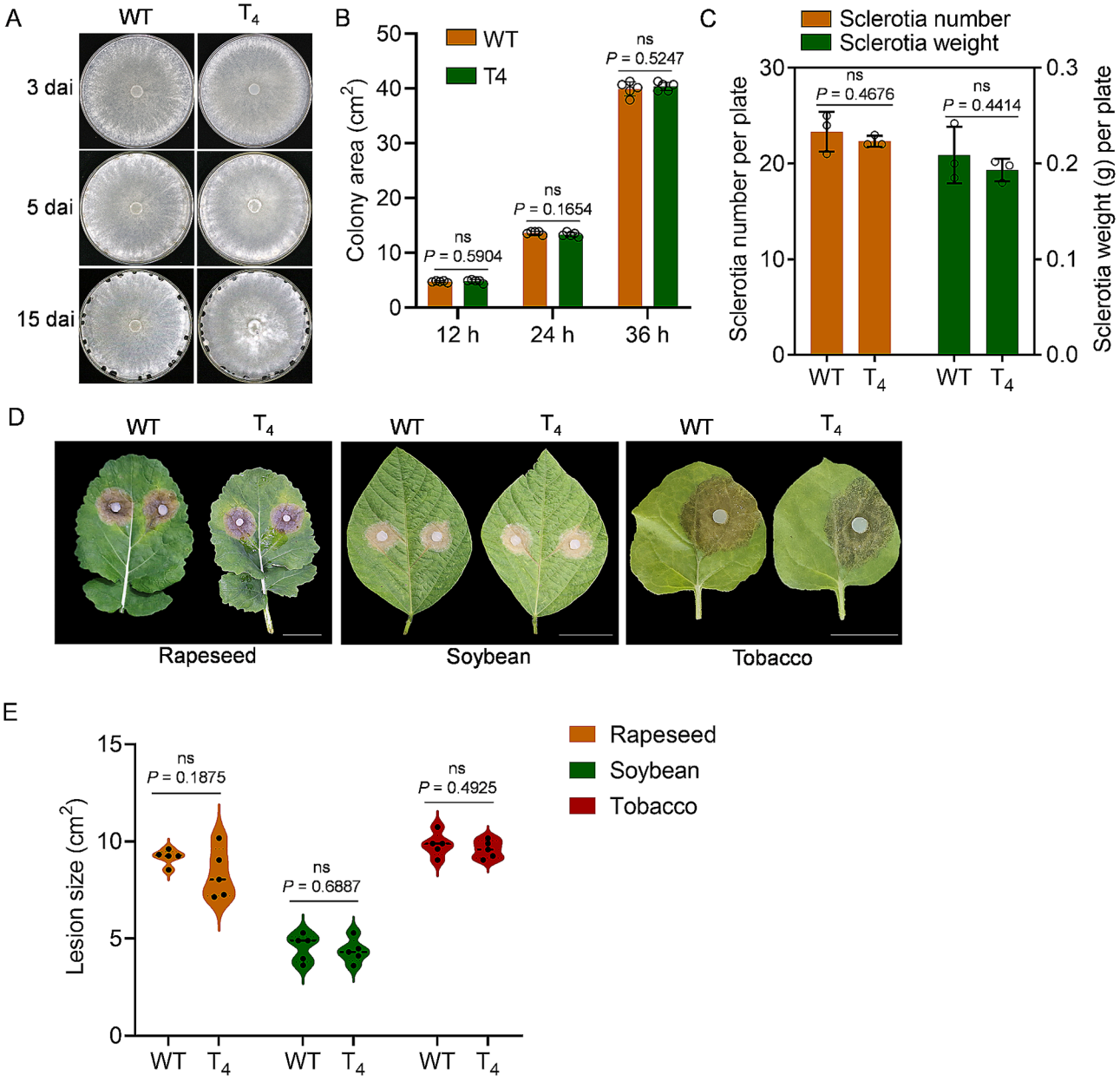

Fig. 5 Characteristics of the T_4 transgenic *S. sclerotiorum*. **A**: Colony morphology and sclerotia formation of wild type and T_4 transgenic *S. sclerotiorum* on PDA medium. WT, wild type strain. **B**: Colony area (cm^2) of wild type and T_4 transgenic *S. sclerotiorum*. Error bars represent SD from three replicates. 'ns' means no significant difference. **C**: Number and mass of sclerotia per petri plate with 90 mm diameter. Error bars represent SD from three replicates. **D**: Pathogenicity of wild type and transgenic *S. sclerotiorum* on leaves of rapeseed, soybean, and tobacco. Lesion size was recorded at 48 hpi. Scale bars, 30 mm. **E**: Evaluation of lesion size (cm^2) produced by transgenic *S. sclerotiorum* and WT strains on leaves of rapeseed, soybean and tobacco. Error bars represent SD from three replicates. 'ns' means no significant difference between WT and T_4 transgenic strains

no discernible impact on the hyphal growth, sclerotia development, and pathogenicity of *S. sclerotiorum*.

OA has been demonstrated experimentally to be a critical virulence factor for *S. sclerotiorum* colonization and *Ss-oah1* is pivotal for OA accumulation [34]. Consequently, *S. sclerotiorum Ss-oah1* was then selected as a target for gene silence analysis to ascertain the viability of FM-mediated-mycelium transformation system. The FM-Sioah1, by loading the *Ss-oah1* gene RNAi construct (pSioah1) onto the surface of FM (Supplementary Fig. 3), was directly transformed with *S. sclerotiorum* mycelium and re-cultured on hygromycin-PDA medium up to T_4 generation. Five hygromycin-resistant transformants were obtained and three genetically modified strains (designated as Sioah1-4, Sioah1-6, and Sioah1-11) with remarkable reduction in *Ss-oah1* expression were selected based on the qRT-PCR analysis (Fig. 6A). Compared to WT, the expression of *Ss-oah1* was reduced to 0.27 in Sioah1-4, 0.31 in Sioah1-6, and 0.41 in Sioah1-11, respectively.

The pathogenicity assay revealed a pronounced reduction in virulence among the *Ss-oah1*-silenced strains relative to WT (Fig. 6B, C; $P<0.0001$). The WT strain produced an average lesion size of approximate 6.04 cm^2 on the rapeseed leaves at 48 hpi, whereas the *Ss-oah1*-silenced strains Sioah1-4, Sioah1-6, and Sioah1-11 produced significantly smaller lesion sizes of 2.24 cm^2, 2.43 cm^2, and 2.32 cm^2, respectively (Fig. 6C). This represented a decrease in lesion size of roughly 63% for the silenced strains compared to WT. Further assessments were carried out to evaluate the OA-producing capacity of the *Ss-oah1*-silenced strains qualitatively and quantitatively. On PDA medium supplemented with bromophenol blue, a colorimetric pH indicator, the WT strain induced color shift from violet to yellow at 2 dai, indicative of OA production. However, the medium inoculated with the transgenic strains exhibited slightly yellow (Fig. 6D), suggesting a significantly diminished production of OA. Quantitative evaluation of OA-producing reduction was confirmed by HPLC analysis, significant

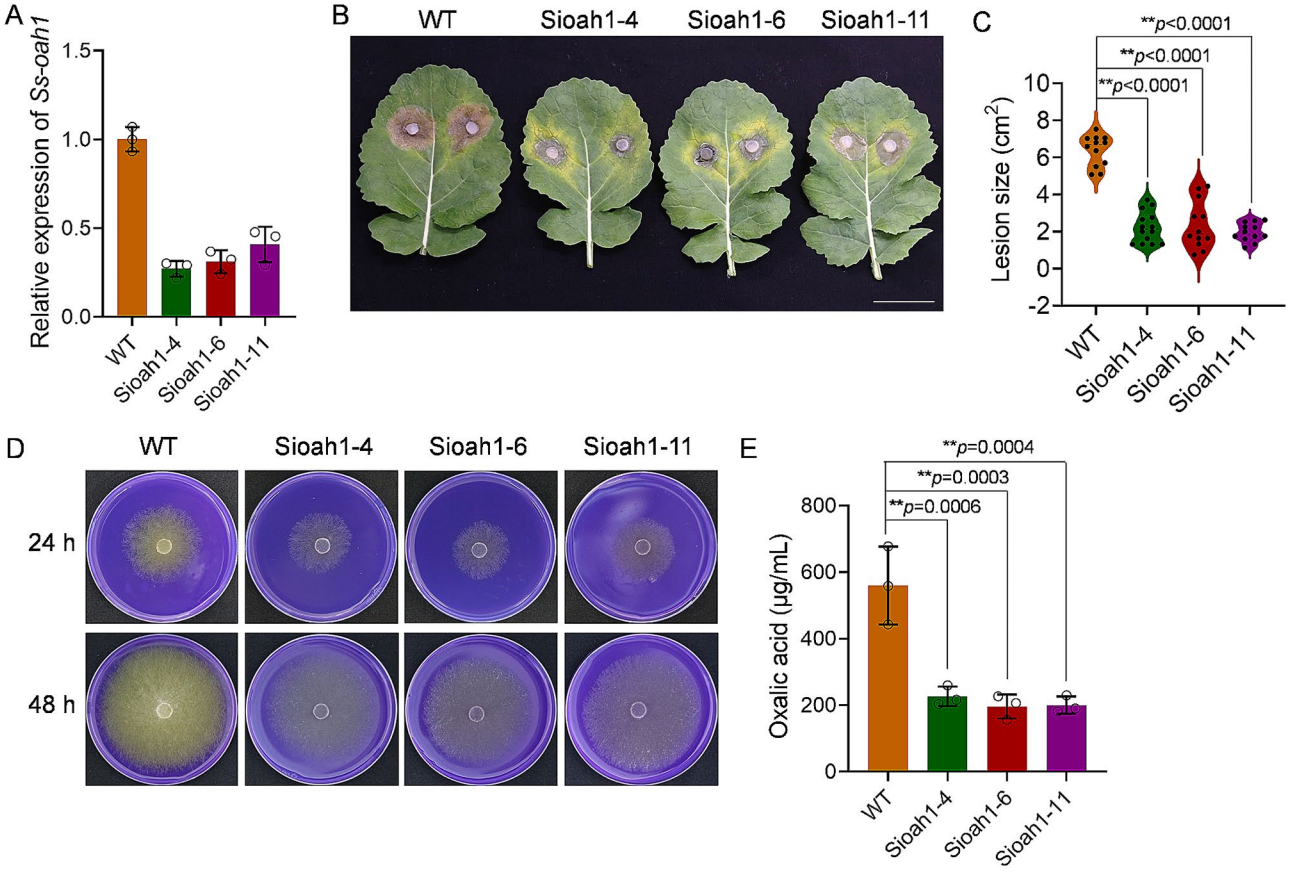

Fig. 6 *Ss-oah1* silencing mediated by FM via mycelium transformation. **A**: Relative expression levels of *Ss-oah1* in different *Ss-oah1*-silenced isolates and wild type strain were determined by qRT-PCR. *Sstubulin* was used as the internal standard. WT, wild type strain. **B**: Pathogenicity of *Ss-oah1*-silenced strains (Sioah1-4, Sioah1-6, and Sioah1-11) on rapeseed leaves. Lesions were recorded at 48 hpi. Scale bars, 30 mm. **C**: Evaluation of lesion size (cm^2) produced by *Ss-oah1*-silenced strains and wild type strains on leaves of rapeseed. **D**: Medium acidification is indicated by color change from violet to yellow. **E**: OA accumulation in PDB. Error bars in (**A**), (**C**) and (**E**) represent SD from three replicates. ** in (**C**) and (**E**) means significant difference between WT and *Ss-oah1* gene-silenced strains

decreased OA content among transgenic strains compared to the WT was detected ($P<0.001$). Specifically, the WT strain accumulated approximate 559.72 μg OA in 1 mL PDB solution, whereas Sioah1-4, Sioah1-6, and Sioah1-11 strains produced markedly lower concentrations of OA, measuring at 226.82 $\mu g \cdot mL^{-1}$, 196.47 $\mu g \cdot mL^{-1}$, and 200.38 $\mu g \cdot mL^{-1}$, respectively (Fig. 6E). These findings indicate that the silencing of *Ss-oah1* effectively reduced the OA-production capacity of the *Ss-oah1*-silencied strains, coincided with the *Ss-oah1* expression level (Fig. 6A). These evidences further reinforce the utility of the FM-mediated genetic transformation system for the elucidation of gene function in *S. sclerotiorum*.

Discussion

Genetic engineering in *S. sclerotiorum* plays a pivotal role in rapidly and directly identifying the pathogenesis genes, thereby facilitating the development of targets for effective disease management. Nonetheless, the primary challenges in genetic engineering of filamentous fungi include low transformation efficiency and intricate and labor-intensive procedural requirements [7]. The pursuit of an efficient genetic transformation system remains an urgent aim and a fundamental prerequisite. This study presents a novel approach employing FM that efficiently deliver exogenous DNAs into the *S. sclerotiorum* genome via direct incubation with the mycelium. This method circumvents the traditional requirement for protoplast preparation and the subsequent recovery process, presenting an innovative strategy for genetic transformation in *S. sclerotiorum* and potentially other filamentous fungi. The FM emerges as a promising tool to surmount the existing obstacles in genetic engineering, thereby facilitating more efficient gene identification processes.

The application of nanomaterials in genetic transformation in plants demonstrate the remarkable advantages of nanomaterials, such as reduced recipient-dependence, high transformation efficiency, excellent biocompatibility, and effective protection of exogenous nucleic acids from nuclease degradation [18, 20, 21]. In current study, we pioneered the transformation of *GFP* into *S. sclerotiorum* cells using FM. While exhibiting high efficiency, AT- and PEG-mediated transformation still required a labor-intensive protoplast preparation and recovery procedure [8, 44]. In *Aspergillus niger*, the direct use of mycelia or conidia as recipients for gene transformation has eliminates the need for extensive recovery and screening steps [45]. Leveraging this reference, we successfully employ FM to transform *GFP* and *Ss-oah1*-silencing plasmid into *S. sclerotiorum* mycelia, as confirmed by qRT-PCR, re-genome sequencing, and PCR confirmation. Consequently, this FM-mediated mycelium transformation platform emerges as a simpler, time-saving, and promising strategy for genetic transformation in *S. sclerotiorum* presenting potential advancements in genetic manipulation for more fungi.

The interaction between the nanomaterials and the exogenous nucleic acids is governed by electrostatic attraction, which not only facilitates transformation but also shields the nuclei acids from nuclease degradation [46, 47]. In the present research, the cationic charge on the surface of the FM was partially neutralized by the anionic charge of exogenous DNA, thereby promoting the tight absorbability of the plasmid DNA to form FM-DNA complexes. We speculated that this may enable the internalization of the DNA into the fungal cells and protect the exogenous DNA from nucleolytic activity within the *S. sclerotiorum* cells. Successful penetration through the fungal cell walls and delivery of FM-DNA complexes into the nucleus is another critical aspect in successful application of this FM-mediated transformation platform. Here, the unique morphology of the FM-DNA complexes likely plays a role in facilitating this process. Future research should aim at elucidating potential structure alterations or pore-forming mechanisms on the cell wall, plasma membrane, or nuclear membrane of the recipient cell.

The successful integration of *GFP* mediated by FM in *S. sclerotiorum* was confirmed by genome-sequencing and validated by PCR analysis. However, the occurrence of random deletions or insertions in the transformant was observed. We speculated that it might be due to the morphological attributes or other characteristics of the FM, which needs further verification. Therefore, effectively controlling the random damage and decreasing the random insertion in our transformation system needs to be further explored to get more effective transformation and avoid the tedious screening for the desired transformants.

Despite the numerous advantages of nanomaterial, the non-cytotoxicity remains a crucial concern when it is employed for genetic transformation [48, 49]. While recognizing the utility, it is imperative to evaluate the potential risks and adverse effects associated with nanotechnology applications [50]. In the present study, the *GFP*-transformed *S. sclerotiorum* strains mediated by the FM grew normally and maintained the pathogenic properties, indicating negligible toxicity from FM. This biological compatibility holds promise for its widespread application in the genetic transformation of filamentous fungi. Despite the apparent biocompatibility of FM, the investigation in the removal or degradation within recipient cell is a worthwhile pursuit.

Considering the diversity of fungal species and the complexity of their cell wall structures, species-specific transformation protocols must be tailored for individual strains. In some instances, the development of entirely novel methods may be imperative to facilitate efficient

transformation [51]. Therefore, further exploration and empirical validation are indispensable to ascertain the general applicability of the present transformation system in other fungi. A more profound understanding of the characteristics of the nanoparticles will accelerate its deployment in filamentous genetic engineering.

Conclusion

In the present study, we have successfully demonstrated the use of FM as a novel carrier for the transgenic transformation in *S. sclerotiorum*. The FM-mediated mycelium transformation circumvents the traditional requirement for protoplast preparation and the subsequent recovery process and exhibits excellent repeatability, efficiency, and high-throughput. This innovative approach represents a significant stride toward achieving tissue-independent delivery of genetic material into the *S. sclerotiorum* cells. By capitalizing on the distinctive properties of nanoparticles, the present system successfully overcomes the inherent challenge posed by the fungal cell wall, presenting a promising tool for advancing genetic manipulation in notable phytopathogenic fungus.

Supplementary Information

The online version contains supplementary material available at https://doi.org/10.1186/s12951-024-02736-6.

Supplementary Material 1

Supplementary Material 2

Author contributions

H. W., W. Q. and Y. D. conceived and designed the research. Y. D., N. Y., Y. L. and J. X. performed experiments. Y. D., H. W., W. Q., K. R., Y. C., and Z. X. Analyzed the data and wrote the manuscript. Z. X. provided suggestions and technical support. All authors contributed to this study, read, and approved the final manuscript.

Funding

The authors thank the financial support from the National Key Research and Development Program of China (2023YFF1000700), the National Natural Science Foundation of China (32372077, 32072021), the Fundamental Research Funds for the Central Universities (SWU120075), and the Natural Science Foundation of Chongqing (CSTB2023NSCQ-MSX0355, CSTB2024NSCQ-MSX0293).

Data availability

We have deposited the sequencing data in the NCBI database, and it has been assigned the Sequence Read Archive (SRA) accession number PRJNA1126013.

Declarations

Ethics approval and consent to participate

Not applicable.

Consent of publication

Not applicable.

Competing interests

The authors declare no competing interests. At the same time, we are also grateful to the tools provided by the Figdraw (www.figdraw.com) platform for drawing Graphical Abstract.

Author details

[1]Integrative Science Center of Germplasm Creation in Western China (Chongqing) Science City, Chongqing and Southwest University, College of Agronomy and Biotechnology, Southwest University, Beibei, Chongqing 400715, China
[2]Academy of Agricultural Sciences, Southwest University, Beibei, Chongqing 400715, China
[3]School of Materials and Energy, Southwest University, Beibei, Chongqing 400715, China

Received: 17 May 2024 / Accepted: 23 July 2024
Published online: 20 August 2024

References

1. Fisher MC, Henk DA, Briggs CJ, Brownstein JS, Madoff LC, McCraw SL, Gurr SJ. Emerging fungal threats to animal, plant and ecosystem health. Nature. 2012;484:186–94.
2. Steinberg G, Gurr SJ. Fungi, fungicide discovery and global food security. Fungal Genet Biol. 2020;144:103476.
3. Manici LM, Bregaglio S, Fumagalli D, Donatelli M. Modelling soil borne fungal pathogens of arable crops under climate change. Int J Biometeorol. 2014;58(10):2071–83.
4. Bolton MD, Thomma BPHJ, Nelson BD. *Sclerotinia Sclerotiorum* (Lib.) De Bary: biology and molecular traits of a cosmopolitan pathogen. Mol Plant Pathol. 2006;7:1–16.
5. Kabbage M, Yarden O, Dickman MB. Pathogenic attributes of *Sclerotinia sclerotiorum*: switching from a biotrophic to necrotrophic lifestyle. Plant Sci. 2015;233:53–60.
6. Xia ST, Xu Y, Hoy RH, Zhang JX, Qin L, Li X. The notorious soilborne pathogenic fungus *Sclerotinia sclerotiorum*: an update on genes studied with mutant analysis. Pathogens. 2019;9:27.
7. Li DD, Tang Y, Lin J, Cai WW. Methods for genetic transformation of filamentous fungi. Microb Cell Fact. 2017;16:168.
8. Liu ZH, Friesen TL. Polyethylene glycol (PEG)-mediated transformation in filamentous fungal pathogens. Methods Mol Biol. 2012;835:365–75.
9. Weld RJ, Eady CC, Ridgway HJ. Agrobacterium-mediated transformation of *Sclerotinia Sclerotiorum*. J Microbiol Methods. 2006;65:202–7.
10. Sanford JC, Smith FD, Russell JA. Optimizing the biolistic process for different biological applications. Methods Enzymol. 1993;217:483–509.
11. Te'o VSJ, Nevalainen KMH. Use of the biolistic particle delivery system to transform fungal genomes. Springer International Publishing; 2015. https://doi.org/10.1007/978-3-319-10142-2_12.
12. Magaña-Ortíz D, Coconi-Linares N, Ortiz-Vazquez E, Fernández F, Loske AM, Gómez-Lim MA. A novel and highly efficient method for genetic transformation of fungi employing shock waves. Fungal Genet Biol. 2013;56:9–16.
13. Rivera AL, Magaña-Ortíz D, Gómez-Lim M, Fernández F, Loske AM. Physical methods for genetic transformation of fungi and yeast. Phys Life Rev. 2014;11:184–203.
14. Yin H, Kanasty RL, Eltoukhy AA, Vegas AJ, Dorkin JR, Anderson DG. Non-viral vectors for gene-based therapy. Nat Rev Genet. 2014;15:541–55.
15. Martin-Ortigosa S, Peterson DJ, Valenstein JS, Lin SY, Trewyn BG, Lyznik LA, Wang K. Mesoporous silica nanoparticle-mediated intracellular cre protein delivery for maize genome editing via loxP site excision. Plant Physiol. 2014;164:537–47.
16. Zhao X, Meng ZG, Wang Y, Chen WJ, Sun CJ, Cui B, Cui JH, Yu ML, Zeng ZH, Guo SD, et al. Pollen magnetofection for genetic modification with magnetic nanoparticles as gene carriers. Nat Plants. 2017;3:956–64.
17. Wang ZP, Zhang ZB, Zheng DY, Zhang TT, Li XL, Zhang C, Yu R, Wei JH, Wu ZY. Efficient and genotype independent maize transformation using pollen transfected by DNA-coated magnetic nanoparticles. J Integr Plant Biol. 2022;64:1145–56.
18. Ben-Haim AE, Feldbaum RA, Belausov E, Zelinger E, Maria R, Nativ-Roth E, Mani KA, Barda O, Sionov E, Mechrez G. DNA delivery to intact plant cells by casein nanoparticles with confirmed gene expression. Adv Funct Mater. 2024;34:2314756.
19. Demirer GS, Zhang H, Goh NS, Pinals RL, Chang R, Landry MP. Carbon nanocarriers deliver siRNA to intact plant cells for efficient gene knockdown. Sci Adv. 2020;6:eaaz0495.

20. Cai Y, Liu ZJ, Wang H, Meng H, Cao YH. Mesoporous silica nanoparticles mediate SiRNA delivery for long-term multi-gene silencing in itact plnats. Adv Sci. 2024;1(19):2301358.
21. Yu P, Zheng XG, Alimi LO, Al-Babili S, Khashab NM. Metal-organic framework-mediated delivery of nucleic acid across intact plant cells. ACS Appl Mater Interfaces. 2024;17(15):18245–51.
22. Jat SK, Bhattacharya J, Sharma MK. Nanomaterial based gene delivery: a promising method for plant genome engineering. J Mater Chem B. 2020;8:4165–75.
23. Vijayakumar PS, Abhilash OU, Khan BM, Prasad BLV. Nanogold-loaded sharp-edged carbon bullets as plant-gene carriers. Adv Funct Mater. 2010;20:2416–23.
24. Naqvi S, Maitra AN, Abdin MZ, Akmal Md, Arora I, Samim Md. Calcium phosphate nanoparticle mediated genetic transformation in plants. J Mater Chem. 2012;22:3500.
25. Mitter N, Worrall EA, Robinson KE, Li P, Jain RG, Taochy C, Fletcher SJ, Carroll BJ, Lu GQM, Xu ZP. Clay nanosheets for topical delivery of RNAi for sustained protection against plant viruses. Nat Plants. 2017;3:16207.
26. Zhang H, Goh NS, Wang JW, Pinals RL, González-Grandío E, Demirer GS, Butrus S, Fakra SC, Del Rio Flores A, Zhai R, et al. Nanoparticle cellular internalization is not required for RNA delivery to mature plant leaves. Nat Nanotechnol. 2022;17:197–205.
27. Wang JW, Cunningham FJ, Goh NS, Boozarpour NN, Pham M, Landry MP. Nanoparticles for protein delivery in planta. Curr Opin Plant Biol. 2021;60:102052.
28. Kwak SY, Giraldo JP, Wong MH, Koman VB, Lew TTS, Ell J, et al. A nanobionic light-emitting plant. Nano Lett. 2017;17:7951–61.
29. Zhang H, Demirer GS, Zhang H, Ye T, Goh NS, Aditham AJ, Cunningham FJ, Fan C, Landry MP. DNA nanostructures coordinate gene silencing in mature plants. Proc Natl Acad Sci U S A. 2019;116(15):7543–8.
30. Li S, Li J, Du M, Deng G, Song Z, Han H. Efficient gene silencing in intact plant cells using siRNA delivered by functional graphene oxide nanoparticles. Angew Chem Int Ed Engl. 2022;61(40):e202210014.
31. Filyak Y, Finiuk N, Mitina N, Bilyk O, Titorenko V, Hrydzhuk O, Zaichenko A, Stoika R. A novel method for genetic transformation of yeast cells using oligoelectrolyte polymeric nanoscale carriers. Biotechniques. 2013;54(1):35–43.
32. Deshmukh K, Ramanan SR, Kowshik M. A novel method for genetic transformation of C. albicans using modified-hydroxyapatite nanoparticles as a plasmid DNA vehicle. Nanoscale Adv. 2019;1(8):3015–22.
33. Zhang XL, Hou SX, Liang MY, Xu JM, Ye MJ, Wang YX, Wen FQ, Xu ZG, Liu SX. Engineering Nanofusiform Iron-doped polydiaminopyridine boost intratumoral penetration for immunogenic cell death-mediated synergistic Photothermal/Chemo therapy. Chem Eng J. 2023;462:142159.
34. Liang XF, Liberti D, Li MY, Kim YT, Hutchens A, Wilson R, Rollins JA. Oxaloacetate acetylhydrolase gene mutants of Sclerotinia Sclerotiorum do not accumulate oxalic acid, but do produce limited lesions on host plants. Mol Plant Pathol. 2015;16(6):559–71.
35. Godoy G, Steadman JR, Dickman MB, Dam R. Use of mutants to demonstrate the role of oxalic acid in pathogenicity of *Sclerotinia sclerotiorum* on *Phaseolus vulgaris*. Physiol MolPlant P. 1990;37:179–91.
36. Leroch M, Mernke D, Koppenhoefer D, Schneider P, Mosbach A, Doehlemann G, Hahn M. Living colors in the gray mold pathogen *Botrytis Cinerea*: codon-optimized genes encoding green fluorescent protein and mCherry, which exhibit bright fluorescence. Appl Environ Microbiol. 2011;77:2887–97.
37. Ding YJ, Mei JQ, Chai YR, Yang WJ, Mao Y, Yan BQ, Yu Y, Disi JO, Rana K, Li JN, et al. *Sclerotinia Sclerotiorum* utilizes host-derived copper for ROS detoxification and infection. PLoS Pathog. 2020;16:e1008919.
38. Braim FS, Razak NNANA, Aziz AA, Dheyab MA, Ismael LQ. Optimization of ultrasonic-assisted approach for synthesizing a highly stable biocompatible bismuth-coated iron oxide nanoparticles using a face-centered central composite design. Ultrason Sonochem. 2023;95:106371–86.
39. Rollins JA. The Sclerotinia Sclerotiorum pac1 gene is required for sclerotial development and virulence. Mol Plant Microbe Interact. 2003;16:785–95.
40. Sambrook J, Fritsch EF, Maniatis T. Molecular cloning: a laboratory manual. 2nd ed. Cold Spring Harbor: Cold Spring Harbor Laboratory Press; 1989.
41. Esher SK, Granek JA, Alspaugh JA. Rapid mapping of insertional mutations to probe cell wall regulation in *Cryptococcus neoformans*. Fungal Genet Biol. 2015;82:9–21.
42. Livak KJ, Schmittgen TD. Analysis of relative gene expression data using real-time quantitative PCR and the 2(-Delta Delta C(T)) method. Methods. 2001;25:402–8.
43. Liu X, Zhang K, Liu Y, Xie Z, Zhang C. Oxalic acid from *Sesbania Rostrata* seed exudates mediates the chemotactic response of *Azorhizobium caulinodans* ORS571 using multiple strategies. Front Microbiol. 2019;10:2727.
44. Jiang DE, Zhu W, Wang YC, Sun C, Zhang KQ, Yang JK. Molecular tools for functional genoics in filamentous fungi: recent advances and new strategies. Biotechnol Adv. 2013;31(8):1562–74.
45. Ozeki K, Kyoya F, Hizume K, Kanda A, Hamachi M, Nunokawa Y. Transformation of intact *aspergillus Niger* by electroporation. Biosci Biotechnol Biochem. 1994;58:2224–7.
46. Zheng M, Jagota A, Semke ED, Diner BA, McLean RS, Lustig SR, Richardson RE, Tassi NG. DNA-assisted dispersion and separation of carbon nanotubes. Nat Mater. 2003;2:338–42.
47. Amar-Lewis E, Azagury A, Chintakunta R, Goldbart R, Traitel T, Prestwood J, Landesman-Milo D, Peer D, Kost J. Quaternized starch-based carrier for siRNA delivery: from cellular uptake to gene silencing. J Control Release. 2014;185:109–20.
48. Sun XD, Yuan XZ, Jia YB, Feng LJ, Zhu FP, Dong SS, Liu JJ, Kong XP, Tian HY, Duan JL, et al. Differentially charged nanoplastics demonstrate distinct accumulation in *Arabidopsis thaliana*. Nat Nanotechnol. 2020;15:755–60.
49. Gao MY, Chang J, Wang ZT, Zhang HT, Wang T. Advances in transport and toxicity of nanoparticles in plants. J Nanobiotechnol. 2023;21:75.
50. Hola K, Zhang Y, Wang Y, Giannelis EP, Zboril R, Rogach AL. Carbon dots—emerging light emitters for bioimaging, cancer therapy and optoelectronics. Nano Today. 2014;9:590–603.
51. van den Berg MA, Maruthachalam KM. Genetic transformation systems in fungi. Genetic Transformation Systems in Fungi. Switzerland: Springer International Publishing; 2015. pp. 3–4.

Publisher's Note